

6-22-2011

Determination of $f_{\bar{s}}/f_{\bar{d}}$ for 7 TeV pp Collisions and a Measurement of the Branching Fraction of the Decay $B_d \rightarrow D-K^+$

Raymond Mountain
Syracuse University

Marina Artuso
Syracuse University

S. Blusk
Syracuse University

Alessandra Borgia
Syracuse University

Follow this and additional works at: <https://surface.syr.edu/phy>

 Part of the [Physics Commons](#)

Recommended Citation

Mountain, Raymond; Artuso, Marina; Blusk, S.; and Borgia, Alessandra, "Determination of $f_{\bar{s}}/f_{\bar{d}}$ for 7 TeV pp Collisions and a Measurement of the Branching Fraction of the Decay $B_d \rightarrow D-K^+$ " (2011). *Physics*. 373.
<https://surface.syr.edu/phy/373>

This Article is brought to you for free and open access by the College of Arts and Sciences at SURFACE. It has been accepted for inclusion in Physics by an authorized administrator of SURFACE. For more information, please contact surface@syr.edu.

Determination of f_s/f_d for 7 TeV pp collisions and a measurement of the branching fraction of the decay $B^0 \rightarrow D^- K^+$

R. Aaij²³, B. Adeva³⁶, M. Adinolfi⁴², C. Adrover⁶, A. Affolder⁴⁸, Z. Ajaltouni⁵, J. Albrecht³⁷, F. Alessio^{6,37}, M. Alexander⁴⁷, G. Alkhazov²⁹, P. Alvarez Cartelle³⁶, A.A. Alves Jr²², S. Amato², Y. Amhis³⁸, J. Amoraal²³, J. Anderson³⁹, R.B. Appleby⁵⁰, O. Aquines Gutierrez¹⁰, L. Arrabito⁵³, A. Artamonov³⁴, M. Artuso^{52,37}, E. Aslanides⁶, G. Auremma^{22,m}, S. Bachmann¹¹, J.J. Back⁴⁴, D.S. Bailey⁵⁰, V. Balagura^{30,37}, W. Baldini¹⁶, R.J. Barlow⁵⁰, C. Barschel³⁷, S. Barsuk⁷, W. Barter⁴³, A. Bates⁴⁷, C. Bauer¹⁰, Th. Bauer²³, A. Bay³⁸, I. Bediaga¹, K. Belous³⁴, I. Belyaev^{30,37}, E. Ben-Haim⁸, M. Benayoun⁸, G. Bencivenni¹⁸, S. Benson⁴⁶, J. Benton⁴², R. Bernet³⁹, M.-O. Bettler^{17,37}, M. van Beuzekom²³, A. Bien¹¹, S. Bifani¹², A. Bizzeti^{17,h}, P.M. Bjørnstad⁵⁰, T. Blake⁴⁹, F. Blanc³⁸, C. Blanks⁴⁹, J. Blouw¹¹, S. Blusk⁵², A. Bobrov³³, V. Bocci²², A. Bondar³³, N. Bondar²⁹, W. Bonivento¹⁵, S. Borghi⁴⁷, A. Borgia⁵², T.J.V. Bowcock⁴⁸, C. Bozzi¹⁶, T. Brambach⁹, J. van den Brand²⁴, J. Bressieux³⁸, S. Brisbane⁵¹, M. Britsch¹⁰, T. Britton⁵², N.H. Brook⁴², A. Büchler-Germann³⁹, A. Bursche³⁹, J. Buytaert³⁷, S. Cadeddu¹⁵, J.M. Caicedo Carvajal³⁷, O. Callot⁷, M. Calvi^{20,j}, M. Calvo Gomez^{35,n}, A. Camboni³⁵, P. Campana^{18,37}, A. Carbone¹⁴, G. Carboni^{21,k}, R. Cardinale^{19,i}, A. Cardini¹⁵, L. Carson³⁶, K. Carvalho Akiba²³, G. Casse⁴⁸, M. Cattaneo³⁷, M. Chatterjee⁵¹, Ph. Charpentier³⁷, N. Chiapolini³⁹, X. Cid Vidal³⁶, P.E.L. Clarke⁴⁶, M. Clemencic³⁷, H.V. Cliff⁴³, J. Closier³⁷, C. Coca²⁸, V. Coco²³, J. Cogan⁶, P. Collins³⁷, F. Constantin²⁸, G. Conti³⁸, A. Contu⁵¹, A. Cook⁴², M. Coombes⁴², G. Corti³⁷, G.A. Cowan³⁸, R. Currie⁴⁶, B. D'Almeida⁷, C. D'Ambrosio³⁷, P. David⁸, P.N.Y. David²³, I. De Bonis⁴, S. De Capua^{21,k}, M. De Cian³⁹, F. De Lorenzi¹², J.M. De Miranda¹, L. De Paula², P. De Simone¹⁸, D. Decamp⁴, M. Deckenhoff⁹, H. Degaudenzi^{38,37}, M. Deissenroth¹¹, L. Del Buono⁸, C. Deplano¹⁵, O. Deschamps⁵, F. Dettori^{15,d}, J. Dickens⁴³, H. Dijkstra³⁷, P. Diniz Batista¹, D. Dossett⁴⁴, A. Dovbnya⁴⁰, F. Dupertuis³⁸, R. Dzhelezian³⁴, C. Eames⁴⁹, S. Easo⁴⁵, U. Egede⁴⁹, V. Egorychev³⁰, S. Eidelman³³, D. van Eijk²³, F. Eisele¹¹, S. Eisenhardt⁶, R. Ekelhof⁹, L. Eklund⁴⁷, Ch. Elsasser³⁹, D.G. d'Entferria^{35,o}, D. Esperante Pereira³⁶, L. Estève⁴³, A. Falabella^{16,e}, E. Fanchini^{20,j}, C. Färber¹¹, G. Fardell⁴⁶, C. Farinelli²³, S. Farry¹², V. Fave³⁸, V. Fernandez Albor³⁶, M. Ferro-Luzzi³⁷, S. Filippov³², C. Fitzpatrick⁴⁶, M. Fontana¹⁰, F. Fontanelli^{19,i}, R. Forty³⁷, M. Frank³⁷, C. Frei³⁷, M. Frosini^{17,f,37}, S. Furcas²⁰, A. Gallas Torreira³⁶, D. Galli^{14,c}, M. Gandelman², P. Gandini⁵¹, Y. Gao³, J.-C. Garnier³⁷, J. Garofoli⁵², L. Garrido³⁵, C. Gaspar³⁷, N. Gauvin³⁸, M. Gersabeck³⁷, T. Gershon⁴⁴, Ph. Ghez⁴, V. Gibson⁴³, V.V. Gligorov³⁷, C. Göbel⁵⁴, D. Golubkov³⁰, A. Golutvin^{49,30,37}, A. Gomes², H. Gordon⁵¹, M. Grabalosa Gándara³⁵, R. Graciani Diaz³⁵, L.A. Granado Cardoso³⁷, E. Graugés³⁵, G. Graziani¹⁷, A. Grecu⁴³, S. Gregson⁴³, B. Gui⁵², E. Gushchin³², Yu. Guz³⁴, T. Gys³⁷, G. Haefeli³⁸, S.C. Haines⁴³, T. Hampson⁴², S. Hansmann-Menzemer¹¹, R. Harji⁴⁹, N. Harnew⁵¹, J. Harrison⁵⁰, P.F. Harrison⁴⁴, J. He⁷, V. Heijne²³, K. Hennessy⁴⁸, P. Henrard⁵, J.A. Hernandez Morata³⁶, E. van Herwijnen³⁷, W. Hofmann¹⁰, K. Holubyev¹¹, P. Hopchev⁴, W. Hulsbergen²³, P. Hunt⁵¹, T. Huse⁴⁸, R.S. Huston¹², D. Hutchcroft⁴⁸, D. Hynds⁴⁷, V. Iakovenko⁴¹, P. Ilten¹², J. Imong⁴², R. Jacobsson³⁷, M. Jahjah Hussein⁵, E. Jans²³, F. Jansen²³, P. Jaton³⁸, B. Jean-Marie⁷, F. Jing³, M. John⁵¹, D. Johnson⁵¹, C.R. Jones⁴³, B. Jost³⁷, S. Kandybel⁴⁰, T.M. Karbach⁹, J. Keaveney¹², U. Kerzel³⁷, T. Ketel²⁴, A. Keune³⁸, B. Khanji⁶, Y.M. Kim⁴⁶, M. Knecht³⁸, S. Koblitz³⁷, P. Koppenburg²³, A. Kozlinskiy²³, L. Kravchuk³², K. Kreplin¹¹, G. Krocker¹¹, P. Krokovny¹¹, F. Kruse⁹, K. Kruzelecki³⁷, M. Kucharczyk^{20,25}, S. Kukulak²⁵, R. Kumar^{14,37}, T. Kvaratskheliya^{30,37}, V.N. La Thi³⁸, D. Lacarrere³⁷, G. Lafferty⁵⁰, A. Lai¹⁵, D. Lambert⁴⁶, R.W. Lambert³⁷, E. Lanciotti³⁷, G. Lanfranchi¹⁸, C. Langenbruch¹¹, T. Latham⁴⁴, R. Le Gac⁶, J. van Leerdam²³, J.-P. Lees⁴, R. Lefevre⁵, A. Leflat^{31,37}, J. Lefrançois⁷, O. Leroy⁶, T. Lesiak²⁵, L. Li³, Y.Y. Li⁴³, L. Li Gioi⁵, M. Lieng⁹, R. Lindner³⁷, C. Linn¹¹, B. Liu³, G. Liu³⁷, J.H. Lopes², E. Lopez Asamar³⁵, N. Lopez-March³⁸, J. Luisier³⁸, F. Machefert⁷, I.V. Makhikhilian^{4,30}, F. Maciuc¹⁰, O. Maev^{29,37}, J. Magnin¹, A. Maier³⁷, S. Malde⁵¹, R.M.D. Mamunur³⁷, G. Manca^{15,d}, G. Mancinelli⁶, N. Mangiafave⁴³, U. Marconi¹⁴, R. Märki³⁸, J. Marks¹¹, G. Martellotti²², A. Martens⁷, L. Martin⁵¹, A. Martín Sánchez⁷, D. Martínez Santos³⁷, A. Massafferri¹, Z. Mathe¹², C. Matteuzzi²⁰, M. Matveev²⁹, E. Maurice⁶, B. Maynard⁵², A. Mazurov^{32,16,37}, G. McGregor⁵⁰, R. McNulty¹², C. Mclean¹⁴, M. Meissner¹¹, M. Merk²³, J. Merkel⁹, R. Messi^{21,k}, S. Miglioranza³⁷, D.A. Milanes^{13,37}, M.-N. Minard⁴, S. Monteil⁵, D. Moran¹², P. Morawski²⁵, J.V. Morris⁴⁵, R. Mountain⁵², I. Mous²³, F. Muheim⁴⁶, K. Müller³⁹, R. Muresan^{28,38}, B. Muryin²⁶, M. Musy³⁵, P. Naik⁴², T. Nakada³⁸, R. Nandakumar⁴⁵, J. Nardulli⁴⁵, M. Nedos⁹, M. Needham⁴⁶, N. Neufeld³⁷, C. Nguyen-Mau^{38,p}, M. Nicol⁷, S. Nies⁹, V. Niess⁵, N. Nikitin³¹, A. Oblakowska-Mucha²⁶, V. Obraztsov³⁴, S. Oggero²³, S. Ogilvy⁴⁷, O. Okhrimenko⁴¹, R. Oldeman^{15,d}, M. Orlandea²⁸, J.M. Otalora Goicochea², B. Pal⁵², J. Palacios³⁹, M. Palutan¹⁸, J. Panman³⁷, A. Papanestis⁴⁵, M. Pappagallo^{13,b}, C. Parkes^{47,37}, C.J. Parkinson⁴⁹, G. Passaleva¹⁷, G.D. Patel⁴⁸, M. Patel⁴⁹, S.K. Paterson⁴⁹, G.N. Patrick⁴⁵, C. Patrignani^{19,i}, C. Pavel-Nicorescu²⁸, A. Pazos Alvarez³⁶, A. Pellegrino²³, G. Penso^{22,l}, M. Pepe Altarelli³⁷, S. Perazzini^{14,c}, D.L. Perego^{20,j}, E. Perez Trigo³⁶, A. Pérez-Calero Yzquierdo³⁵, P. Perret⁵, M. Perrin-Terrin⁶, G. Pessina²⁰, A. Petrella^{16,37}, A. Petrolini^{19,i}, B. Pie Valls³⁵, B. Pietrzyk⁴, T. Pilar⁴⁴, D. Pinci²², R. Plackett⁴⁷, S. Playfer⁴⁶, M. Plo Casasus³⁶, G. Polok²⁵, A. Poluektov^{44,33}, E. Polcarpo², D. Popov¹⁰, B. Popovici²⁸, C. Potterat³⁵, A. Powell⁵¹, T. du Pree²³, V. Pugatch⁴¹, A. Puig Navarro³⁵, W. Qian⁵², J.H. Rademacker⁴², B. Rakotomiramanana³⁸, I. Raniuk⁴⁰, G. Raven²⁴, S. Redford⁵¹, M.M. Reid⁴⁴, A.C. dos Reis¹, S. Ricciardi⁴⁵, K. Rinnert⁴⁸, D.A. Roa Romero⁵, P. Robbe⁷, E. Rodrigues⁴⁷, F. Rodrigues², C. Rodriguez Cobo³⁶, P. Rodriguez Perez³⁶, G.J. Rogers⁴³, V. Romanovsky³⁴, J. Rouvinet³⁸, T. Ruf⁴⁷, H. Ruiz³⁵, G. Sabatino^{21,k}, J.J. Saborido Silva³⁶, N. Sagidova²⁹, P. Sail⁴⁷, B. Saitta^{15,d}, C. Salzmann³⁹, M. Sannino^{19,i}, R. Santacesaria²², R. Santinelli³⁷, E. Santovetti^{21,k}, M. Sapunov⁶, A. Sarti^{18,l}, C. Satriano^{22,m}, A. Satta²¹, M. Savrie^{16,e}, D. Savrina³⁰, P. Schaack⁴⁹, M. Schiller¹¹, S. Schleich⁹, M. Schmelling¹⁰, B. Schmidt³⁷, O. Schneider³⁸, A. Schopper³⁷, M.-H. Schune⁷, R. Schwemmer³⁷, A. Sciubba^{18,l}, M. Seco³⁶, A. Semennikov³⁰, K. Senderowska²⁶, N. Serra³⁹, J. Serrano⁶, P. Seyfert¹¹, B. Shao³, M. Shapkin³⁴, I. Shapoval^{40,37}, P. Shatalov³⁰, Y. Shcheglov²⁹, T. Shears⁴⁸, L. Shekhtman³³, O. Shevchenko⁴⁰, V. Shevchenko³⁰, A. Shires⁴⁹, R. Silva Coutinho⁵⁴, H.P. Skottowe⁴³, T. Skwarnicki⁵², A.C. Smith³⁷, N.A. Smith⁴⁸, K. Sobczak⁵, F.J.P. Soler⁴⁷, A. Solomin⁴², F. Soomro⁴⁹, B. Souza De Paula², B. Spaan⁹, A. Sparkes⁴⁶,

P. Spradlin⁴⁷, F. Stagni³⁷, S. Stahl¹¹, O. Steinkamp³⁹, S. Stoica²⁸, S. Stone^{52,37}, B. Storaci²³, U. Straumann³⁹, N. Styles⁴⁶, S. Swientek⁹, M. Szczekowski²⁷, P. Szczypka³⁸, T. Szumlak²⁶, S. T'Jampens⁴, E. Teodorescu²⁸, F. Teubert³⁷, C. Thomas^{51,45}, E. Thomas³⁷, J. van Tilburg¹¹, V. Tisserand⁴, M. Tobin³⁹, S. Topp-Joergensen⁵¹, M.T. Tran³⁸, A. Tsaregorodtsev⁶, N. Tuning²³, A. Ukleja²⁷, P. Urquijo⁵², U. Uwer¹¹, V. Vagnoni¹⁴, G. Valenti¹⁴, R. Vazquez Gomez³⁵, P. Vazquez Regueiro³⁶, S. Vecchi¹⁶, J.J. Velthuis⁴², M. Veltri^{17,g}, K. Vervink³⁷, B. Viaud⁷, I. Videau⁷, X. Vilasis-Cardona^{35,n}, J. Visniakov³⁶, A. Vollhardt³⁹, D. Voong⁴², A. Vorobyev²⁹, H. Voss¹⁰, K. Wacker⁹, S. Wandernoth¹¹, J. Wang⁵², D.R. Ward⁴³, A.D. Webber⁵⁰, D. Websdale⁴⁹, M. Whitehead⁴⁴, D. Wiedner¹¹, L. Wiggers²³, G. Wilkinson⁵¹, M.P. Williams^{44,45}, M. Williams⁴⁹, F.F. Wilson⁴⁵, J. Wishahi⁹, M. Witek²⁵, W. Witzeling³⁷, S.A. Wotton⁴³, K. Wyllie³⁷, Y. Xie⁴⁶, F. Xing⁵¹, Z. Yang³, R. Young⁴⁶, O. Yushchenko³⁴, M. Zavertyaev^{10,a}, L. Zhang⁵², W.C. Zhang¹², Y. Zhang³, A. Zhelezov¹¹, L. Zhong³, E. Zverev³¹, A. Zvyagin³⁷.

¹Centro Brasileiro de Pesquisas Físicas (CBPF), Rio de Janeiro, Brazil

²Universidade Federal do Rio de Janeiro (UFRJ), Rio de Janeiro, Brazil

³Center for High Energy Physics, Tsinghua University, Beijing, China

⁴LAPP, Université de Savoie, CNRS/IN2P3, Annecy-Le-Vieux, France

⁵Clermont Université, Université Blaise Pascal, CNRS/IN2P3, LPC, Clermont-Ferrand, France

⁶CPPM, Aix-Marseille Université, CNRS/IN2P3, Marseille, France

⁷LAL, Université Paris-Sud, CNRS/IN2P3, Orsay, France

⁸LPNHE, Université Pierre et Marie Curie, Université Paris Diderot, CNRS/IN2P3, Paris, France

⁹Fakultät Physik, Technische Universität Dortmund, Dortmund, Germany

¹⁰Max-Planck-Institut für Kernphysik (MPIK), Heidelberg, Germany

¹¹Physikalisches Institut, Ruprecht-Karls-Universität Heidelberg, Heidelberg, Germany

¹²School of Physics, University College Dublin, Dublin, Ireland

¹³Sezione INFN di Bari, Bari, Italy

¹⁴Sezione INFN di Bologna, Bologna, Italy

¹⁵Sezione INFN di Cagliari, Cagliari, Italy

¹⁶Sezione INFN di Ferrara, Ferrara, Italy

¹⁷Sezione INFN di Firenze, Firenze, Italy

¹⁸Laboratori Nazionali dell'INFN di Frascati, Frascati, Italy

¹⁹Sezione INFN di Genova, Genova, Italy

²⁰Sezione INFN di Milano Bicocca, Milano, Italy

²¹Sezione INFN di Roma Tor Vergata, Roma, Italy

²²Sezione INFN di Roma La Sapienza, Roma, Italy

²³Nikhef National Institute for Subatomic Physics, Amsterdam, Netherlands

²⁴Nikhef National Institute for Subatomic Physics and Vrije Universiteit, Amsterdam, Netherlands

²⁵Henryk Niewodniczanski Institute of Nuclear Physics Polish Academy of Sciences, Cracow, Poland

²⁶Faculty of Physics & Applied Computer Science, Cracow, Poland

²⁷Soltan Institute for Nuclear Studies, Warsaw, Poland

²⁸Horia Hulubei National Institute of Physics and Nuclear Engineering, Bucharest-Magurele, Romania

²⁹Petersburg Nuclear Physics Institute (PNPI), Gatchina, Russia

³⁰Institute of Theoretical and Experimental Physics (ITEP), Moscow, Russia

³¹Institute of Nuclear Physics, Moscow State University (SINP MSU), Moscow, Russia

³²Institute for Nuclear Research of the Russian Academy of Sciences (INR RAN), Moscow, Russia

³³Budker Institute of Nuclear Physics (SB RAS) and Novosibirsk State University, Novosibirsk, Russia

³⁴Institute for High Energy Physics (IHEP), Protvino, Russia

³⁵Universitat de Barcelona, Barcelona, Spain

³⁶Universidad de Santiago de Compostela, Santiago de Compostela, Spain

³⁷European Organization for Nuclear Research (CERN), Geneva, Switzerland

³⁸Ecole Polytechnique Fédérale de Lausanne (EPFL), Lausanne, Switzerland

³⁹Physik-Institut, Universität Zürich, Zürich, Switzerland

⁴⁰NSC Kharkiv Institute of Physics and Technology (NSC KIPT), Kharkiv, Ukraine

⁴¹Institute for Nuclear Research of the National Academy of Sciences (KINR), Kyiv, Ukraine

⁴²H.H. Wills Physics Laboratory, University of Bristol, Bristol, United Kingdom

⁴³Cavendish Laboratory, University of Cambridge, Cambridge, United Kingdom

⁴⁴Department of Physics, University of Warwick, Coventry, United Kingdom

⁴⁵STFC Rutherford Appleton Laboratory, Didcot, United Kingdom

⁴⁶School of Physics and Astronomy, University of Edinburgh, Edinburgh, United Kingdom

⁴⁷School of Physics and Astronomy, University of Glasgow, Glasgow, United Kingdom

⁴⁸Oliver Lodge Laboratory, University of Liverpool, Liverpool, United Kingdom

⁴⁹Imperial College London, London, United Kingdom

⁵⁰School of Physics and Astronomy, University of Manchester, Manchester, United Kingdom

⁵¹Department of Physics, University of Oxford, Oxford, United Kingdom

⁵²Syracuse University, Syracuse, NY, United States

⁵³CC-IN2P3, CNRS/IN2P3, Lyon-Villeurbanne, France, associated member

⁵⁴Pontifícia Universidade Católica do Rio de Janeiro (PUC-Rio), Rio de Janeiro, Brazil, associated to ²

^a*P.N. Lebedev Physical Institute, Russian Academy of Science (LPI RAS), Moscow, Russia*

^b*Università di Bari, Bari, Italy*

^c*Università di Bologna, Bologna, Italy*

^d*Università di Cagliari, Cagliari, Italy*

^e*Università di Ferrara, Ferrara, Italy*

^f*Università di Firenze, Firenze, Italy*

^g*Università di Urbino, Urbino, Italy*

^h*Università di Modena e Reggio Emilia, Modena, Italy*

ⁱ*Università di Genova, Genova, Italy*

^j*Università di Milano Bicocca, Milano, Italy*

^k*Università di Roma Tor Vergata, Roma, Italy*

^l*Università di Roma La Sapienza, Roma, Italy*

^m*Università della Basilicata, Potenza, Italy*

ⁿ*LIFAELS, La Salle, Universitat Ramon Llull, Barcelona, Spain*

^o*Institució Catalana de Recerca i Estudis Avançats (ICREA), Barcelona, Spain*

^p*Hanoi University of Science, Hanoi, Viet Nam*

(The LHCb Collaboration)

The relative abundance of the three decay modes $B^0 \rightarrow D^- K^+$, $B^0 \rightarrow D^- \pi^+$ and $B_s^0 \rightarrow D_s^- \pi^+$ produced in 7 TeV pp collisions at the LHC is determined from data corresponding to an integrated luminosity of 35 pb^{-1} . The branching fraction of $B^0 \rightarrow D^- K^+$ is found to be $\mathcal{B}(B^0 \rightarrow D^- K^+) = (2.01 \pm 0.18^{\text{stat}} \pm 0.14^{\text{sys}}) \times 10^{-4}$. The ratio of fragmentation fractions f_s/f_d is determined through the relative abundance of $B_s^0 \rightarrow D_s^- \pi^+$ to $B^0 \rightarrow D^- K^+$ and $B^0 \rightarrow D^- \pi^+$, leading to $f_s/f_d = 0.253 \pm 0.017 \pm 0.017 \pm 0.020$, where the uncertainties are statistical, systematic, and theoretical respectively.

PACS numbers: 12.38.Qk, 13.60.Le, 13.87.Fh

Knowledge of the production rate of B_s^0 mesons is required to determine any B_s^0 branching fraction. This rate is determined by the $b\bar{b}$ production cross-section and the fragmentation probability f_s , which is the fraction of B_s^0 mesons amongst all weakly-decaying bottom hadrons. Similarly the production rate of B^0 mesons is driven by the fragmentation probability f_d . The measurement of the branching fraction of the rare decay $B_s^0 \rightarrow \mu^+ \mu^-$ is a prime example where improved knowledge of f_s/f_d is needed to reach the highest sensitivity in the search for physics beyond the Standard Model [1]. The ratio f_s/f_d has not yet been measured at LHC.

The branching fraction ratio $B_s^0 \rightarrow D_s^- \pi^+ / B^0 \rightarrow D^- K^+$ is dominated by contributions from colour-allowed tree-diagram amplitudes and is therefore theoretically well understood. In contrast, the ratio $B_s^0 \rightarrow D_s^- \pi^+ / B^0 \rightarrow D^- \pi^+$ can be measured with a smaller statistical uncertainty due to the greater yield of the B^0 mode, but suffers from an additional theoretical uncertainty due to the contribution from a W -exchange diagram. Both ratios are exploited here to measure f_s/f_d according to the equations [2, 3]

$$\frac{f_s}{f_d} = 0.0743 \times \frac{\tau_{B_d}}{\tau_{B_s}} \times \left[\frac{1}{\mathcal{N}_a \mathcal{N}_F} \frac{\epsilon_{D^- K^+}}{\epsilon_{D_s^- \pi^+}} \frac{N_{D_s^- \pi^+}}{N_{D^- K^+}} \right], \quad (1)$$

and

$$\frac{f_s}{f_d} = 0.982 \times \frac{\tau_{B_d}}{\tau_{B_s}} \times \left[\frac{1}{\mathcal{N}_a \mathcal{N}_F \mathcal{N}_E} \frac{\epsilon_{D^- \pi^+}}{\epsilon_{D_s^- \pi^+}} \frac{N_{D_s^- \pi^+}}{N_{D^- \pi^+}} \right]. \quad (2)$$

Here ϵ_X is the selection efficiency of decay X (includ-

ing the branching fraction of the D decay mode used to reconstruct it) and N_X is the observed number of decays of this type. Inclusion of charge conjugate modes is implied throughout. The term \mathcal{N}_a parameterises non-factorizable SU(3)-breaking effects; \mathcal{N}_F is the ratio of the form factors; \mathcal{N}_E is an additional correction term to account for the W -exchange diagram in the $B^0 \rightarrow D^- \pi^+$ decay. Their values [2, 3] are $\mathcal{N}_a = 1.00 \pm 0.02$, $\mathcal{N}_F = 1.24 \pm 0.08$, and $\mathcal{N}_E = 0.966 \pm 0.075$. The latest world average [4] is used for the B meson lifetime ratio $\tau_{B_s}/\tau_{B_d} = 0.973 \pm 0.015$. Other numerical factors have negligible associated uncertainties [5].

The observed yields of these three decay modes in 35 pb^{-1} of data collected with the LHCb detector in the 2010 running period are used to measure f_s/f_d averaged over the LHCb acceptance and to improve the current measurement of the branching fraction of the $B^0 \rightarrow D^- K^+$ decay mode [6].

The LHCb experiment [7] is a single-arm spectrometer, designed to study B decays at the LHC, with a pseudo-rapidity acceptance of $2 < \eta < 5$ for charged tracks. The first trigger level allows the selection of events with B hadronic decays using the transverse energy of hadrons measured in the calorimeter system. The event information is subsequently sent to a software trigger, implemented in a dedicated processor farm, which performs a final online selection of events for later offline analysis. The tracking system determines the momenta of B decay products with a precision of $\delta p/p = 0.35\text{--}0.5\%$. Two Ring Imaging Cherenkov (RICH) detectors allow charged kaons and pions to be distinguished in the momentum

range 2–100 GeV/c.

The three decay modes, $B^0 \rightarrow D^-(K^+\pi^-\pi^-)\pi^+$, $B^0 \rightarrow D^-(K^+\pi^-\pi^-)K^+$ and $B_s^0 \rightarrow D_s^-(K^+K^-\pi^-)\pi^+$, are topologically identical and therefore can be selected using identical geometric and kinematic criteria, thus minimizing efficiency differences between them. Events are selected at the first trigger stage by requiring a hadron with transverse energy greater than 3.6 GeV in the calorimeter. The second, software, stage [8, 9] requires a two, three, or four track secondary vertex with a high sum p_T of the tracks, significant displacement from the primary interaction, and at least one track with exceptionally high p_T , large displacement from the primary interaction, and small fit χ^2 .

The decays of B mesons can be distinguished from background using variables such as the p_T and impact parameter χ^2 with respect to the primary interaction of the B , D , and the final state particles. In addition the vertex quality of the B and D candidates, the B lifetime, and the angle between the B momentum vector and the vector joining the B production and decay vertices are used in the selection. The D lifetime and flight distance are not used in the selection because the lifetimes of the D_s^- and D^- differ by about a factor of two.

The final event sample is selected using the gradient boosted decision tree technique [10]. The selection is trained on a mixture of simulated $B^0 \rightarrow D^-\pi^+$ decays and combinatorial background selected from the sidebands of the data mass distributions. The distributions of the input variables for data and simulated signal events show excellent agreement, justifying the use of simulated events in the training procedure.

Subsequently, D^- (D_s^-) candidates are identified by requiring the invariant mass under the $K\pi\pi$ ($KK\pi$) hypothesis to fall within the selection window 1870_{-40}^{+24} (1969_{-40}^{+24}) MeV/c². The final $B^0 \rightarrow D^-\pi^+$ and $B_s^0 \rightarrow D_s^-\pi^+$ subsamples consist of events that pass a particle identification (PID) criterion on the bachelor particle, based on the difference in log-likelihood between the charged pion and kaon hypotheses (DLL) of $\text{DLL}(K - \pi) < 0$. The $B^0 \rightarrow D^-K^+$ subsample consists of events with $\text{DLL}(K - \pi) > 5$. Events not satisfying either condition are not used.

The relative efficiency of the selection procedure is evaluated for all decay modes using simulated events. As the analysis is only sensitive to relative efficiencies, the impact of differences between data and simulation is small. The relative efficiencies are $\epsilon_{D^-\pi^+}/\epsilon_{D^-K^+} = 1.221 \pm 0.021$, $\epsilon_{D^-K^+}/\epsilon_{D_s^-\pi^+} = 0.917 \pm 0.020$, and $\epsilon_{D^-\pi^+}/\epsilon_{D_s^-\pi^+} = 1.120 \pm 0.025$, where the errors are due to the limited size of the simulated event samples.

The relative yields of the three decay modes are extracted from unbinned extended maximum likelihood fits to the mass distributions. The signal mass shape is described by an empirical model derived from simulated events. The mass distribution in the simulation exhibits

non-Gaussian tails on either side of the signal. The tail on the right-hand side is due to non-Gaussian detector effects and modelled with a Crystal Ball (CB) function [11]. A similar tail is present on the left-hand side of the peak. In addition, the low mass tail contains a second contribution due to events where hadrons have radiated photons that are not reconstructed. The sum of these contributions is modelled with a second CB function. The peak values of these two CB functions are constrained to be identical.

Various backgrounds have to be considered, in particular the crossfeed between the D^- and D_s^- channels, and the contamination in both samples from $\Lambda_b \rightarrow \Lambda_c^+\pi^-$ decays, where $\Lambda_c^+ \rightarrow pK^-\pi^+$. The D_s^- contamination in the D^- data sample is reduced by loose PID requirements, $\text{DLL}(K - \pi) < 10$ and $\text{DLL}(K - \pi) > 0$, for the pions and kaons from D decays, respectively. The resulting efficiency to reconstruct $B_s^0 \rightarrow D_s^-\pi^+$ as background is evaluated, using simulated events, to be 30 times smaller than for $B^0 \rightarrow D^-\pi^+$ and 150 times smaller than for $B^0 \rightarrow D^-K^+$ within the B^0 and D^- signal mass windows. Taking into account the lower production fraction of B_s^0 mesons, this background is negligible.

The contamination from Λ_c decays is estimated in a similar way. However, different approaches are used for the B^0 and B_s^0 decays. A contamination of approximately 2% under the $B^0 \rightarrow D^-\pi^+$ mass peak and below 1% under the $B^0 \rightarrow D^-K^+$ peak is found, and therefore no explicit $\text{DLL}(p - \pi)$ criterion is needed. The Λ_c background in the B_s^0 sample is, on the other hand, large enough that it can be fitted for directly.

A prominent peaking background to $B^0 \rightarrow D^-K^+$ is $B^0 \rightarrow D^-\pi^+$, with the pion misidentified as a kaon. The small $\pi \rightarrow K$ misidentification rate is compensated by the larger branching fraction, resulting in similar event yields. This background is modelled by obtaining a clean $B^0 \rightarrow D^-\pi^+$ sample from the data and reconstructing it under the $B^0 \rightarrow D^-K^+$ mass hypothesis. The resulting mass shape depends on the momentum distribution of the bachelor particle. The momentum distribution after the $\text{DLL}(K - \pi) > 5$ requirement can be found by considering the PID performance as a function of momentum. This is obtained using a sample of D^{*+} decays, and is illustrated in Fig. 1. The mass distribution is reweighted using this momentum distribution to reproduce the $B^0 \rightarrow D^-\pi^+$ mass shape following the DLL cut.

The combinatorial background consists of events with random pions and kaons, forming a fake D^- or D_s^- candidate, as well as real, D^- or D_s^- mesons that combine with a random pion or kaon. The combinatorial background is modelled with an exponential shape.

Other background components originate from partially reconstructed B^0 and B_s^0 decays. In $B^0 \rightarrow D^-\pi^+$ these originate from $B^0 \rightarrow D^{*+}\pi^+$ and $B^0 \rightarrow D^-\rho^+$ decays, which can also be backgrounds for $B^0 \rightarrow D^-K^+$ in the case of a misidentified bachelor pion. In

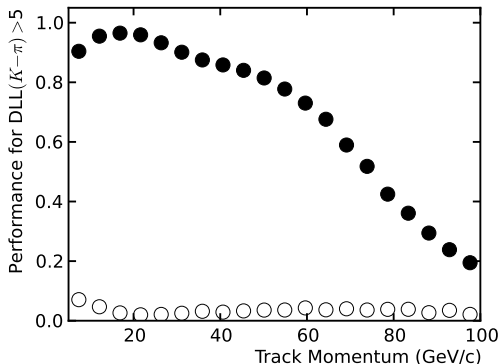


FIG. 1. Probability, as a function of momentum, to correctly identify a kaon (full circles) and to wrongly identify a pion as a kaon (open circles) when requiring $DLL(K - \pi) > 5$. The data are taken from a calibration sample of $D^* \rightarrow D(K\pi)\pi$ decays; the statistical uncertainties are too small to display.

$B^0 \rightarrow D^- K^+$ there is additionally background from $B^0 \rightarrow D^{*-} K^+$ decays. The invariant mass distributions for the partially reconstructed and misidentified backgrounds are taken from large samples of simulated events, reweighted according to the mass hypothesis of the signal being fitted and the DLL cuts.

For $B_s^0 \rightarrow D_s^- \pi^+$, the $B^0 \rightarrow D^- \pi^+$ background peaks under the signal with a similar shape. In order to suppress this peaking background, PID requirements are placed on both kaon tracks. The kaon which has the same sign in the $B_s^0 \rightarrow D_s^- \pi^+$ and $B^0 \rightarrow D^- \pi^+$ decays is required to satisfy $DLL(K - \pi) > 0$, while the other kaon in the D_s^+ decay is required to satisfy $DLL(K - \pi) > 5$. Because of the similar shape, a Gaussian constraint is applied to the yield of this background. The central value of this constraint is computed from the $\pi \rightarrow K$ misidentification rate. The $\Lambda_b \rightarrow \Lambda_c^+ \pi^-$ background shape is obtained from simulated events, reweighted according to the PID efficiency, and the yield allowed to float in the fit. Finally, the relative size of the $B_s^0 \rightarrow D_s^- \rho^+$ and $B_s^0 \rightarrow D_s^{*-} \pi^+$ backgrounds is constrained to the ratio of the $B^0 \rightarrow D^- \rho^+$ and $B^0 \rightarrow D^{*-} \pi^+$ backgrounds in the $B^0 \rightarrow D^- \pi^+$ fit, with an uncertainty of 20% to account for potential SU(3) symmetry breaking effects.

The free parameters in the likelihood fits to the mass distributions are the event yields for the different event types, *i.e.* the combinatorial background, partially reconstructed background, misidentified contributions, the signal, as well as the peak value of the signal shape. In addition the combinatoric background shape is left free in the $B^0 \rightarrow D^- \pi^+$ and $B_s^0 \rightarrow D_s^- \pi^+$ fits, and the signal width is left free in the $B^0 \rightarrow D^- \pi^+$ fit. In the $B_s^0 \rightarrow D_s^- \pi^+$ and $B^0 \rightarrow D^- K^+$ fits the signal width is fixed to the value from the $B^0 \rightarrow D^- \pi^+$ fit, corrected by the ratio of the signal widths for these modes in simulated events.

The fits to the full $B^0 \rightarrow D^- \pi^+$, $B^0 \rightarrow D^- K^+$, and $B_s^0 \rightarrow D_s^- \pi^+$ data samples are shown in Fig. 2. The resulting $B^0 \rightarrow D^- \pi^+$ and $B^0 \rightarrow D^- K^+$ event yields are 4103 ± 75 and 252 ± 21 , respectively. The number of misidentified $B^0 \rightarrow D^- \pi^+$ events under the $B^0 \rightarrow D^- K^+$ signal as obtained from the fit is 131 ± 19 . This agrees with the number expected from the total number of $B^0 \rightarrow D^- \pi^+$ events, corrected for the misidentification rate determined from the PID calibration sample, of 145 ± 5 . The $B_s^0 \rightarrow D_s^- \pi^+$ event yield is 670 ± 34 .

The stability of the fit results has been investigated using different cut values for both the PID requirement

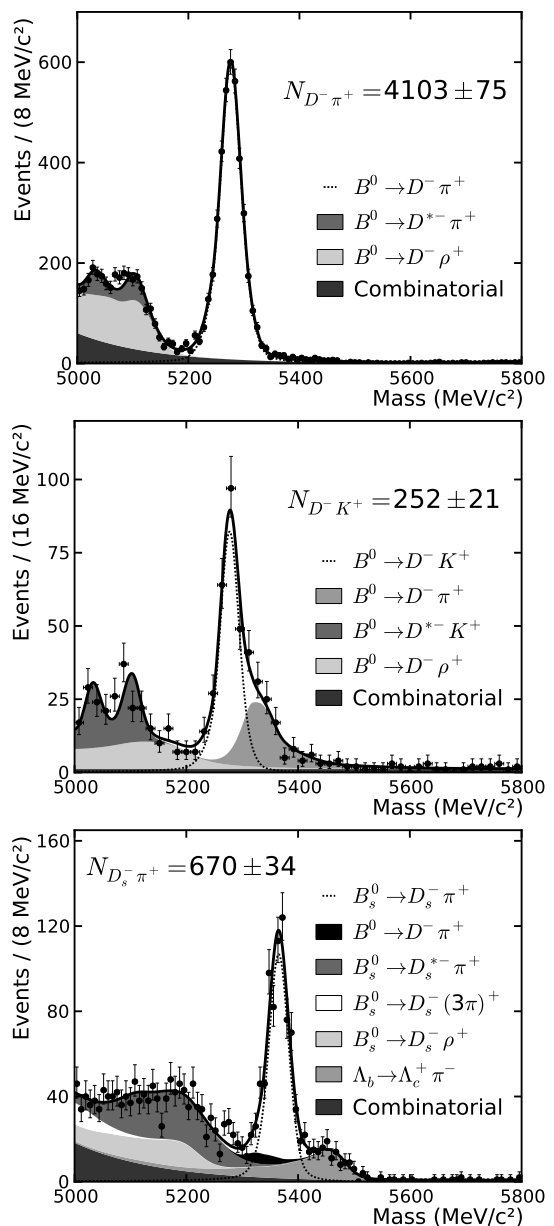


FIG. 2. Mass distributions of the $B^0 \rightarrow D^- \pi^+$, $B^0 \rightarrow D^- K^+$, and $B_s^0 \rightarrow D_s^- \pi^+$ candidates (top to bottom). The indicated components are described in the text.

TABLE I. Experimental systematic uncertainties for the $\mathcal{B}(B^0 \rightarrow D^- K^+)$ and the two f_s/f_d measurements.

	$\mathcal{B}(B^0 \rightarrow D^- K^+)$	f_s/f_d
PID calibration	2.5%	1.0%/2.5%
Fit model	2.8%	2.8%
Trigger simulation	2.0%	2.0%
$\mathcal{B}(B^0 \rightarrow D^- \pi^+)$	4.9%	
$\mathcal{B}(D_s^+ \rightarrow K^+ K^- \pi^+)$		4.9%
$\mathcal{B}(D^+ \rightarrow K^- \pi^+ \pi^+)$		2.2%
τ_{B_s}/τ_{B_d}		1.5%

on the bachelor particle and for the multivariate selection variable. In all cases variations are found to be small in comparison to the statistical uncertainty.

The relative branching fractions are obtained by correcting the event yields by the corresponding efficiency factors; the dominant correction comes from the PID efficiency. The dominant source of systematic uncertainty is the knowledge on the $B^0 \rightarrow D^- \pi^+$ branching fraction (for the $B^0 \rightarrow D^- K^+$ branching fraction measurement) and the knowledge of the D^- and D_s^- branching fractions (for the f_s/f_d measurement). An important source of systematic uncertainty is the knowledge of the PID efficiency as a function of momentum, which is needed to reweight the mass distribution of the $B^0 \rightarrow D^- \pi^+$ decay under the kaon hypothesis for the bachelor track. This enters in two ways: firstly as an uncertainty on the correction factors, and secondly as part of the systematic uncertainty, since the shape for the misidentified backgrounds relies on correct knowledge of the PID efficiency as a function of momentum. The f_s/f_d measurement using $B^0 \rightarrow D^- K^+$ and $B_s^0 \rightarrow D_s^- \pi^+$ is more robust against PID uncertainties, since the final states have the same number of kaons and pions.

Other systematics are due to limited simulated event samples (affecting the relative selection efficiencies), neglecting the $\Lambda_b \rightarrow \Lambda_c^+ \pi^-$ and $B_s^0 \rightarrow D_s^- \pi^+$ backgrounds in the $B^0 \rightarrow D^- \pi^+$ fits, and the limited accuracy of the trigger simulation. The sources of systematic uncertainty are summarized in Tab. I.

The efficiency corrected ratio of $B^0 \rightarrow D^- \pi^+$ and $B^0 \rightarrow D^- K^+$ yields is combined with the world average of the $B^0 \rightarrow D^- \pi^+$ [12] branching ratio to give

$$\mathcal{B}(B^0 \rightarrow D^- K^+) = (2.01 \pm 0.18 \pm 0.14) \times 10^{-4}. \quad (3)$$

The first uncertainty is statistical and the second systematic.

The theoretically cleaner measurement of f_s/f_d uses $B^0 \rightarrow D^- K^+$ and $B_s^0 \rightarrow D_s^- \pi^+$ and is made according to Eq. 1. Accounting for the exclusive D branching fractions $\mathcal{B}(D^+ \rightarrow K^- \pi^+ \pi^+) = (9.14 \pm 0.20)\%$ [13] and $\mathcal{B}(D_s^+ \rightarrow K^- K^+ \pi^+) = (5.50 \pm 0.27)\%$ [14], the value of f_s/f_d is

found to be

$$f_s/f_d = 0.250 \pm 0.024^{\text{stat}} \pm 0.017^{\text{syst}} \pm 0.017^{\text{theor}}, \quad (4)$$

where the first uncertainty is statistical, the second systematic, and the third theoretical. The theoretical uncertainty is dominated by the form factor ratio. The statistical uncertainty is dominated by the yield of the $B^0 \rightarrow D^- K^+$ mode.

The statistically more precise but theoretically less clean measurement of f_s/f_d uses $B^0 \rightarrow D^- \pi^+$ and $B_s^0 \rightarrow D_s^- \pi^+$ and is, from Eq. 2,

$$f_s/f_d = 0.256 \pm 0.014^{\text{stat}} \pm 0.019^{\text{syst}} \pm 0.026^{\text{theor}}. \quad (5)$$

The two values for f_s/f_d can be combined into a single value, taking all correlated uncertainties into account. The value of f_s/f_d is :

$$f_s/f_d = 0.253 \pm 0.017^{\text{stat}} \pm 0.017^{\text{syst}} \pm 0.020^{\text{theor}}. \quad (6)$$

In summary, with 35 pb⁻¹ of data collected using the LHCb detector during the 2010 LHC operation at a centre-of-mass energy of 7 TeV, the branching fraction of the Cabibbo-suppressed B^0 decay mode $B^0 \rightarrow D^- K^+$ has been measured with better precision than the current world average. Additionally, two measurements of the f_s/f_d production fraction are performed from the relative yields of $B_s^0 \rightarrow D_s^- \pi^+$ with respect to $B^0 \rightarrow D^- K^+$ and $B^0 \rightarrow D^- \pi^+$. These values of f_s/f_d are in good agreement with the values determined at LEP and at the Tevatron [4].

ACKNOWLEDGMENTS

We express our gratitude to our colleagues in the CERN accelerator departments for the excellent performance of the LHC. We thank the technical and administrative staff at CERN and at the LHCb institutes, and acknowledge support from the National Agencies: CAPES, CNPq, FAPERJ and FINEP (Brazil); CERN; NSFC (China); CNRS/IN2P3 (France); BMBF, DFG, HGF and MPG (Germany); SFI (Ireland); INFN (Italy); FOM and NWO (Netherlands); SCSR (Poland); ANCS (Romania); MinES of Russia and Rosatom (Russia); MICINN, XUNGAL and GENCAT (Spain); SNSF and SER (Switzerland); NAS Ukraine (Ukraine); STFC (United Kingdom); NSF (USA). We also acknowledge the support received from the ERC under FP7 and the Région Auvergne.

-
- [1] Aaij, R. *et al.* (LHCb Collaboration). *Phys. Lett. B*, 699:330, 2011. arXiv:1103.2465[hep-ex].
[2] R. Fleischer, N. Serra, and N. Tuning. *Phys. Rev.*, D83:014017, 2011. arXiv:1012.2784[hep-ph].

- [3] R. Fleischer, N. Serra, and N. Tuning. *Phys. Rev.*, D82:034038, 2010. arXiv:1004.3982[hep-ph].
- [4] D. Asner et al. arXiv:1010.1589[hep-ex], 2010.
- [5] Here the more accurate value for the kaon form factor, $f_K = 156.1$ MeV, is used compared to the approximate value $f_K = 160$ MeV used in Ref. [3].
- [6] Abe, K. et al. (BELLE Collaboration). *Phys. Rev. Lett.*, 87:111801, 2001. arXiv:0104051[hep-ex].
- [7] A. A. Alves Jr. et al. (LHCb Collaboration). *JINST*, 3:S08005, 2008.
- [8] V. V. Gligorov. LHCb-PUB-2011-003.
- [9] M. Williams et al. LHCb-PUB-2011-002.
- [10] A. Hoecker et al. *PoS*, ACAT:040, 2007.
- [11] T. Skwarnicki. DESY F31-86-02, 1986.
- [12] K. Nakamura et al. *J. Phys. G*, 37(075021), 2010.
- [13] Dobbs, S. et al. (CLEO Collaboration). *Phys. Rev.*, D76:112001, 2007. arXiv:0709.3783[hep-ex].
- [14] Alexander, J. P. et al. (CLEO Collaboration). *Phys. Rev. Lett.*, 100:161804, 2008. arXiv:0801.0680[hep-ex].